Macromolecular Research, Vol. 14, No. 2, pp 146-154 (2006)

Crystallization and Melting Behavior of Silica Nanoparticles and Poly(ethylene 2,6-naphthalate) Hybrid Nanocomposites

Jun Young Kim, Seong Hun Kim*, and Seong Wook Kang

Department of Fiber & Polymer Engineering, Center for Advanced Functional Polymers, Hanyang University, Seoul 133-791, Korea

Jin-Hae Chang

Department of Polymer Science and Engineering, Kumoh National Institute of Technology, Gumi 730-701, Korea

Seon Hoon Ahn

R&D Center, Hyundai Engineering Plastic Co., Ltd., Chungnam 343-856, Korea

Received September 14, 2005; Revised January 16, 2006

Abstract: Organic and inorganic hybrid nanocomposites based on poly(ethylene 2,6-naphthalate) (PEN) and silica nanoparticles were prepared by a melt blending process. In particular, polymer nanocomposites consisting mostly of cheap conventional polyesters with very small quantities of inorganic nanoparticles are of great interest from an industrial perspective. The crystallization behavior of PEN/silica hybrid nanocomposites depended significantly on silica content and crystallization temperature. The activation energy of crystallization for PEN/silica hybrid nanocomposites was decreased by incorporating a small quantity of silica nanoparticles. Double melting behavior was observed in PEN/silica hybrid nanocomposites, and the equilibrium melting temperature decreased with increasing silica content. The fold surface free energy of PEN/silica hybrid nanocomposites decreased with increasing silica content. The work of chain folding (q) for PEN was estimated as 7.28×10^{-20} J per molecular chain fold, while the q values for the PEN/silica 0.9 hybrid nanocomposite was 3.71×10^{-20} J, implying that the incorporation of silica nanoparticles lowers the work required to fold the polymer chains.

Keywords: chain folding, crystallization, melting, nanocomposites, nanoparticles, poly(ethylene 2,6-naphthalate) (PEN), silica.

Introduction

As the state of the art in material science and technology has rapidly advanced, extensive research and development has been performed on high-performance polymers for targeted applications in various industrial fields. Furthermore, a number of efforts to develop high-performance polymers with the benefit of nanotechnology have been made, investigating polymer nanocomposites by incorporation of nano-reinforcements into the polymer matrix, in fields ranging from the scientific to the industrial.[1-6] In recent years, polymer nanocomposites consisting of organic polymers and inorganic nanoparticles have attracted considerable attention because they have significantly improved mechanical, thermal, electrical, and gas barrier properties; the dimensional stability of the polymers is also improved, even with small quantities of nanoparticles.[1-6] This has resulted in their potential applications as advanced materials for the aerospace, automotive, electric, and electronics industries.[1-3] Currently, four processing techniques are commonly used to incorporate inorganic nanoparticles into the polymer matrix for the fabrication of inorganic nanoparticles-reinforced polymer nanocomposites: direct mixing, *in situ* polymerization, solution mixing or film casting, and melt compounding.[7-9] Of these methods, melt compounding is a simpler and more effective process compared with the other processing techniques, particularly from an economic point of view and an industrial perspective. Thus, this technique may hold promise for use in large-scale industrial applications.

The mechanical properties of polymers or nanocomposites are influenced by their morphology, which is affected by their crystallization kinetics. Recently, organic-inorganic hybrid nanocomposites, using nanoparticles incorporated into the polymer matrix to enhance their mechanical properties and

*Corresponding Author. E-mail: kimsh@hanyang.ac.kr

crystallization behavior, have been prepared.[10,11] The crystallization behavior of polymers or nanocomposites and their crystallization kinetics, as a function of the processing conditions, are of great importance in polymer processing, particularly for the effective analysis and design of processing operations. For this reason, the crystallization behavior and structural development of polymer nanocomposites reinforced with nanoparticles should be analyzed to fully realize their potential application in thermoplastic matrix-based polymer nanocomposites. In addition, the processing of polymer composites involves complex deformation behaviors,[12-14] which may affect the nucleation and crystallization behavior of the polymer nanocomposites. It is therefore important to characterize the nucleation and crystallization behavior of the polymer nanocomposites to optimize the process conditions.

In this research, inorganic-organic hybrid nanocomposites consisting of silica nanoparticles and poly(ethylene 2,6-naphthalate) (PEN) were prepared by a melt blending process. The crystallization and melting behavior of PEN/silica hybrid nanocomposites was investigated using isothermal crystallization analysis, and the effect of silica nanoparticles on PEN/silica hybrid nanocomposites is discussed.

Experimental

Materials and Preparation. The thermoplastic polymer used was PEN, with an intrinsic viscosity of 0.93 dL/g, supplied by Hyo Sung Co., Korea. The nanoparticles used were the hydrophilic fumed silica (primary particle size: 7 nm; surface area: 290 m^2/g; purity: 99.8%), purchased from Sigma Aldrich Co. All the materials were dried at 110 °C *in vacuo* for at least 24 h before use to minimize the effects of moisture. PEN and silica hybrid nanocomposites were prepared by melt processing in a Haake Rheomix 600 internal mixer (Gebr. HAAKE GmbH, Germany) at 275 °C for 5 min, with a fixed rotor speed of 60 rpm. For fabrication of PEN/silica hybrid nanocomposites, the PEN was melt-blended with the incorporation of various silica concentrations in the polymer matrix: 0.3, 0.5, 0.7, and 0.9 wt%, respectively.

Characterization. The thermal behavior of the PEN/silica hybrid nanocomposites was measured with a TA Instrument 2010 differential scanning calorimeter (DSC) over the temperature range from 30 to 290 °C under nitrogen, with a scanning rate of 10 °C/min. For the isothermal crystallization experiments, the samples were first heated to 295 °C at a heating rate of 10 °C/min under nitrogen, and maintained at that temperature for 5 min to eliminate any previous thermal history. Then the samples were quenched, employing a cooling rate of 100 °C/min down to the desired crystallization temperatures (in the range 200 to 240 °C), and maintained until crystallization was completed, during which time the heat flow for isothermal crystallization was recorded as a function of time. The samples isothermally crystallized at a set crystallization temperature were then heated to 295 °C at a heating rate of 10 °C/min. Thermogravimetric analysis of the PEN/silica hybrid nanocomposites was performed using a TA Instrument SDF-2960 thermogravimetric analyzer (TGA) under a nitrogen atmosphere, over the temperature range from 30 to 800 °C at a heating rate of 10 °C/min. The wide angle X-ray diffraction (WAXD) measurements were performed using a Rigaku Denki X-ray diffractometer with Ni-filltered CuKα X-rays (λ=0.1542 nm). The diffracting intensities were recorded at steps of 2θ=0.05° over the range of 5° < 2θ < 40°. Dynamic mechanical analysis of the PEN/silica hybrid nanocomposites was performed with a TA Instrument Q-800 dynamic mechanical analyzer (DMA), using a tensile mode at a fixed frequency of 1 Hz over the temperature range from 30 to 250 °C, at a heating rate of 5 °C/min.

Results and Discussion

Thermal Properties. The thermal stability of polymer composites is one of the most important factors for polymer processing and polymer applications. Results from the TGA thermograms of the PEN/silica hybrid nanocomposites as a function of silica content at a heating rate of 10 °C/min under a nitrogen atmosphere are shown in Table I. It can be seen that both the initial decomposition temperature and the temperature at the maximum rate of thermal decomposition on the incorporation of silica nanoparticles into the PEN matrix. In addition, the residual yields of the PEN/silica hybrid nanocomposites increased with increasing silica content. This result demonstrates that the thermal stability of PEN/silica hybrid nanocomposites is improved by the incorporation of silica nanoparticles.

As the processing of polymer nanocomposites involves complex deformation behaviors, which may affect the nucleation and crystallization behavior of the polymer nanocomposites, it is important to characterize the nucleation and crystallization behavior of polymer nanocomposites to optimize the process conditions. Analysis of the crystallization behavior of polymer nanocomposites reinforced with inorganic nanoparticles would make it possible to realize their potential applications in many fields of industry. DSC results

Table I. Thermal Behavior of PEN/Silica Hybrid Nanocomposites as a Function of Silica Content

Materials	T_i [a] (°C)	T_{10} [b] (°C)	T_{60} [b] (°C)	T_{dm} [c] (°C)	W_{800} [d] (%)
PEN	383.5	414.2	448.3	436.9	16.2
PEN/Silica 0.5	386.4	417.3	450.0	439.9	22.2
PEN/Silica 0.9	391.5	421.9	452.0	441.2	25.5

[a]Initial decomposition temperature in TGA at a heating rate of 10 °C/min. [b]Decomposition temperatures at 10 and 60% weight loss, respectively. [c]Decomposition temperature at the maximum decomposition rate. [d]Residual yield in TGA at 800 °C.

Table II. Thermal Behavior of PEN/Silica Hybrid Nanocomposites as a Function of Silica Content

Materials	T_g [a] (°C)	T_m [a] (°C)	ΔH_m [a] (J/g)	T_c [b] (°C)	ΔT [c] (°C)
PEN	119.2	275.8	45.3	199.3	76.5
PEN/silica 0.3	119.5	275.7	43.2	212.5	63.2
PEN/silica 0.5	119.7	274.3	38.4	214.4	59.9
PEN/silica 0.7	120.5	273.1	38.1	218.9	54.2
PEN/silica 0.9	121.1	272.9	39.5	219.8	53.1

[a]Values obtained from DSC heating traces at 5 °C/min. [b]Crystallization temperature measured from DSC cooling traces at 5 °C/min. [c]Degree of supercooling, $\Delta T = T_m - T_c$.

for the PEN/silica hybrid nanocomposites as a function of silica content, employing a scanning rate of 10 °C/min under nitrogen, are shown in Table II. The incorporation of silica nanoparticles slightly increased the glass transition temperature (T_g) and slightly decreased the melting temperature (T_m) of the PEN/silica hybrid nanocomposites. The increase in crystallization temperature of the PEN/silica hybrid nanocomposites with increasing silica content, together with the fact that PEN/silica hybrid nanocomposites have a lower degree of supercooling ($\Delta T = T_m - T_c$) for crystallization with increasing silica content, suggests that the silica nanoparticles can effectively act as nucleating agents in the PEN/silica hybrid nanocomposites. Therefore, it can be deduced that the incorporation of silica nanoparticles effectively enhances the crystallization of the PEN matrix through heterogeneous nucleation.

Crystallization Behavior. Isothermal crystallization exotherms for the PEN/silica hybrid nanocomposites as a function of silica content, and isothermal crystallization exotherms as a function of crystallization temperature are shown in Figures 1 and 2, respectively. As the crystallization temperature increased, the isothermal crystallization exothermal peaks shifted to longer times, implying that the crystallization rate decreased with increasing crystallization temperature. In contrast, as the silica content increased, the isothermal crystallization exothermal peaks shifted to shorter times, indicating faster crystallization rates with increasing silica concentration. The relative degree of crystallinity (X_t) at various crystallization times can be defined as the ratio of the area of the exothermic peak at time t to the total measured area of crystallization. Assuming that the relative degree of crystallinity increased with increasing time, the isothermal crystallization kinetics of PEN and the PEN/silica hybrid nanocomposites were analyzed using the Avrami equation:[15,16]

$$1 - X_t = \exp[-k(t - t_s)^n] \quad (1)$$

where X_t is the relative degree of crystallinity; k is the rate constant; t is the crystallization time; t_s is the initial time of crystallization, and n is the Avrami exponent that is correlated

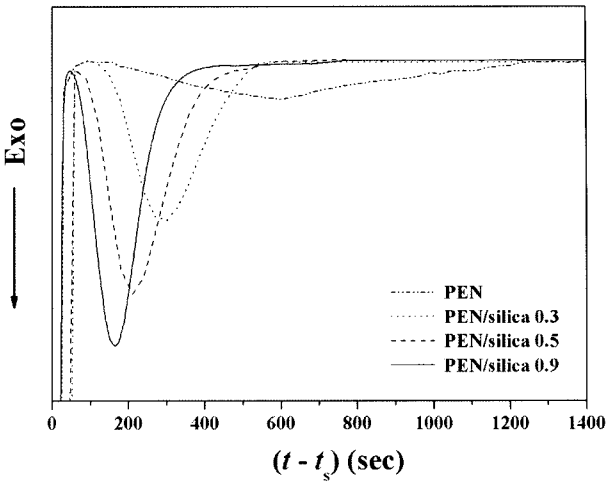

Figure 1. Isothermal crystallization exotherms for PEN/silica hybrid nanocomposites as a function of silica content at an isothermal crystallization temperature of 210 °C.

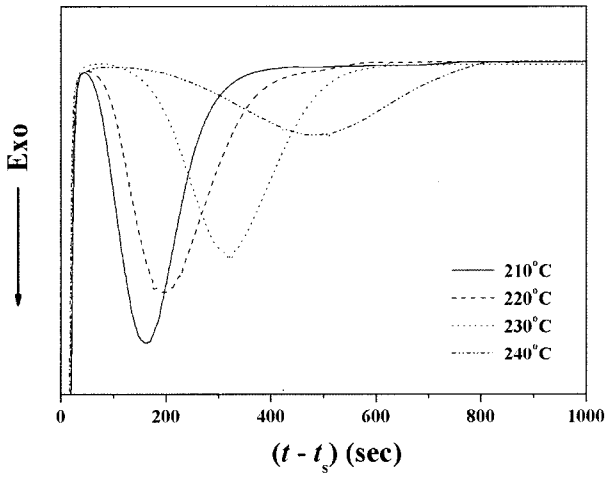

Figure 2. Isothermal crystallization exotherms for PEN/silica 0.9 hybrid nanocomposite as a function of isothermal crystallization temperature.

with the nucleation mechanism and crystal growth. Values of n and k were calculated from the slope and intercept of the plots of $\log[-\ln(1 - X_t)]$ versus $\log(t - t_s)$. Moreover, the half time of crystallization ($t_{1/2}$), one of the important factors describing isothermal crystallization kinetics, can be estimated from eq. (2) using the values of n and k obtained from the Avrami plot. In general, a lower $t_{1/2}$ implies a higher crystallization rate.

$$t_{1/2} = \left(\frac{\ln 2}{k}\right)^{1/n} \quad (2)$$

The dependence of the kinetic parameters on the isothermal crystallization temperature and the silica nanoparticles is shown in Table III. As the crystallization temperature increa-

Table III. Kinetic Parameters for PEN and PEN/Silica Hybrid Nanocomposites During Isothermal Crystallization

Materials	T_c (°C)	n	k (min^{-1})	$t_{1/2}$ (min)
PEN	200	1.7963	7.24×10^{-2}	3.52
	210	1.6364	4.42×10^{-2}	5.38
	220	1.5959	2.87×10^{-2}	7.35
	230	1.7797	1.12×10^{-2}	10.16
	240	1.8140	5.06×10^{-3}	15.07
PEN/silica 0.9	200	2.7120	6.02×10^{-2}	2.46
	210	2.8257	2.86×10^{-2}	3.09
	220	2.8432	2.32×10^{-2}	3.30
	230	4.3036	4.52×10^{-4}	5.50
	240	3.2011	9.88×10^{-4}	7.75

sed, the $t_{1/2}$ value increased and the $\tau_{1/2}$ value decreased. In addition, it can be seen that the incorporation of silica nanoparticles accelerates crystallization of the PEN matrix through heterogeneous nucleation, resulting in a higher crystallization rate. Assuming that the crystallization process is thermally activated, the crystallization rate parameter (K) can be expressed by using the Arrhenius equation as follows:[17,18]

$$K^{1/n} = k_0 \exp(-E_a/RT_c) \quad (3)$$

where k_0 is a temperature independent pre-exponential factor; R is the universal gas constant, and ΔE_a is the crystallization activation energy, which consists of the transport activation energy and the nucleation activation energy. The activation energy for isothermal crystallization can be determined from the slope of the plot of $(1/n)\ln K$ versus $1/T_c$ as shown in Figure 3. The ΔE_a values for PEN and the PEN/silica 0.9 hybrid nanocomposite were 71.18 and 55.87 kJ/mol, respectively. In the presence of 0.9 wt% silica nanoparticles, the ΔE_a values for the PEN/silica hybrid nanocomposite decreased, indicating that the incorporation of silica nanoparticles into the PEN matrix induces more heterogeneous nucleation, causing a lower ΔE_a value.

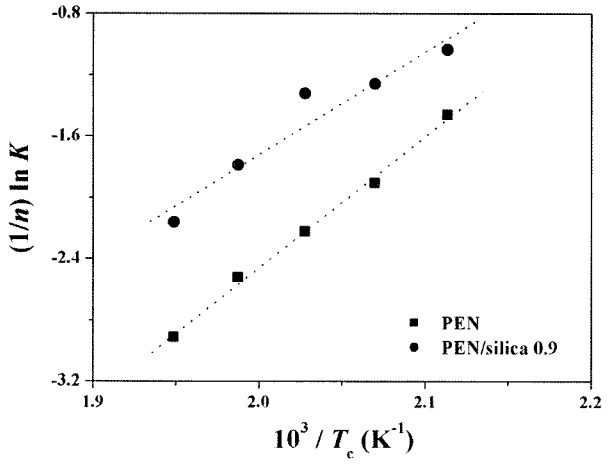

Figure 3. Activation energies for the isothermal crystallization of PEN and PEN/silica 0.9 hybrid nanocomposite.

Melting Behavior. DSC heating traces for PEN and PEN/silica hybrid nanocomposites after the completion of isothermal crystallization at different crystallization temperatures, and then heating from the crystallization temperature to 295 °C at a heating rate of 10 °C/min are shown in Figure 4. PEN and the PEN/silica hybrid nanocomposites exhibited double melting peaks in the DSC heating traces for crystallization temperature up to 230 °C. As the crystallization temperature increased, the lower-temperature melting peaks gradually shifted to higher temperatures, and eventually merged into a single peak at a crystallization temperature of 240 °C. This result indicates that the isothermal crystallization temperature influences the melting behavior of PEN/silica hybrid nanocomposites. In most semicrystalline polymers, as well as in copolymers and blends, multiple melting peaks have been observed during DSC scans. Many investigations have been made into the origin of multiple melting behavior in

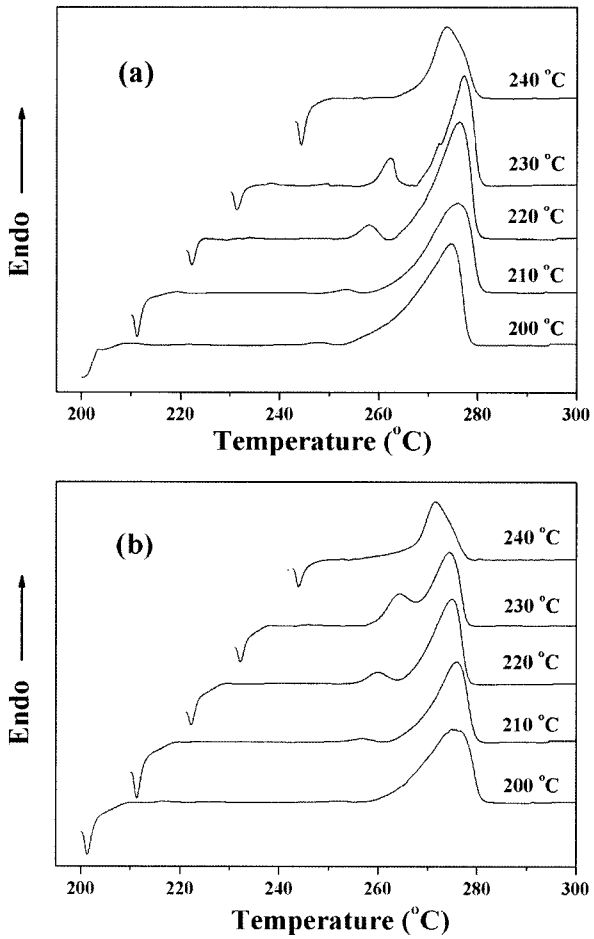

Figure 4. DSC heating traces after the completion of isothermal crystallization for (a) PEN and (b) the PEN/silica 0.7 hybrid nanocomposite.

semicrystalline polymers, copolymers, and polymer blends.[19-23] Various factors such as a change in morphology, orientation effects, the presence of more than one crystal modification, and melting-recrystallization-remelting processes occurring during DCS scans, have influenced multiple melting behaviors. The perfection of the crystalline, or high-temperature melting peaks increased with crystallization temperature, which was confirmed by the fact that the higher-temperature melting peaks shifted to higher temperatures with higher crystallization temperature. Relatively imperfect crystals would be formed at lower crystallizations, and would melt at a lower temperature. The melting-recrystallization-remelting mechanism proposes that original imperfect thin crystals or lamellae in the polymers could melt and recrystallize to form crystals of higher perfection during DSC scans.[24] Supaphol[25] has reported similar observations of multiple melting behaviors, suggesting that the lower-temperature melting peak corresponded to the melting of the primary crystallites formed, and the higher-temperature melting peak corresponded to the melting of the recrystallized crystallites, formed during the DSC heating scan. Wide-angle X-ray diffraction (WAXD) patterns for the PEN/silica hybrid nanocomposites of a given crystallization temperature and time are shown in Figure 5. The position of the observed crystalline peak of the PEN/silica hybrid nanocomposites after isothermal crystallization was unchanged with crystallization temperature and time. This result suggests that the double melting behavior observed in PEN/silica hybrid nanocomposites is attributable to different lamellae thickness distribution as a consequence of the melting-recrystallization process during DSC scans.

Equilibrium Melting Temperature. According to the theoretical relation suggested by Hoffman and Weeks,[26] the equilibrium melting temperature of polymers can be derived from the following equation for the plot of the melting temperature (T_m) versus the isothermal crystallization temperature (T_c):

$$T_m = T_m^0\left(1-\frac{1}{\gamma}\right)+\frac{T_c}{\gamma} \quad (4)$$

where γ is the ratio of the initial to the final lamellar thickness and T_m^0 is the equilibrium melting temperature. The equilibrium melting temperature is obtained from the intersection of the Hoffman-Weeks plot with the line $T_m=T_c$. Hoffman-Weeks plots for PEN and the PEN/silica hybrid nanocomposites at various silica concentrations are shown in Figure 6. The T_m^0 values of the PEN/silica nanocomposites decreased with increasing silica content, which may be attributed to the formation of less perfect spherulites in the PEN/silica hybrid nanocomposites as a result of the strong heterogeneous nucleation effect of the silica nanoparticles. For the polypropylene (PP)/montmorillonite (MMT) nanocomposite system, a large number of nuclei formed by the strong nucleation effect of the MMT resulted in many spherulites existing in a limited space within the nanocomposites,

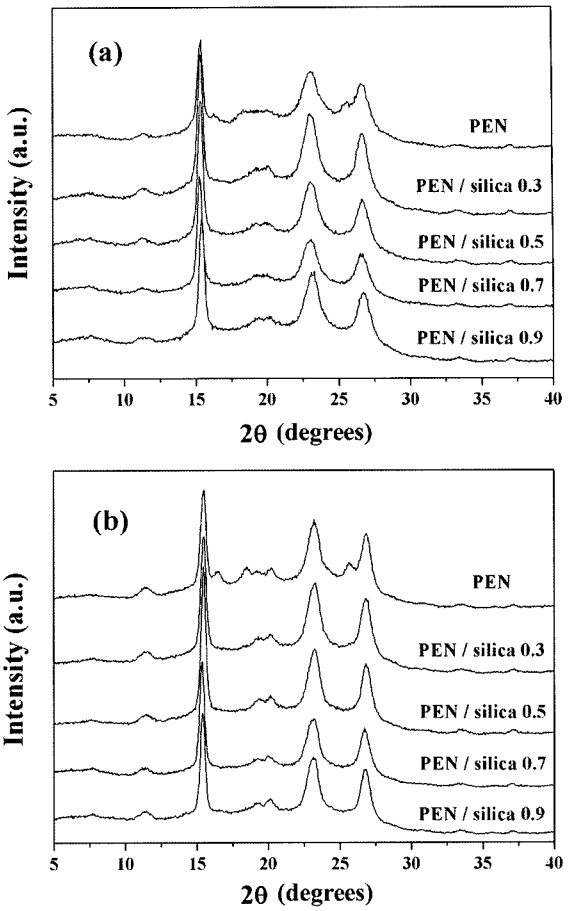

Figure 5. WAXD patterns for PEN/silica hybrid nanocomposites as a function of silica content at isothermal crystallization temperatures of (a) 200 °C and (b) 240 °C.

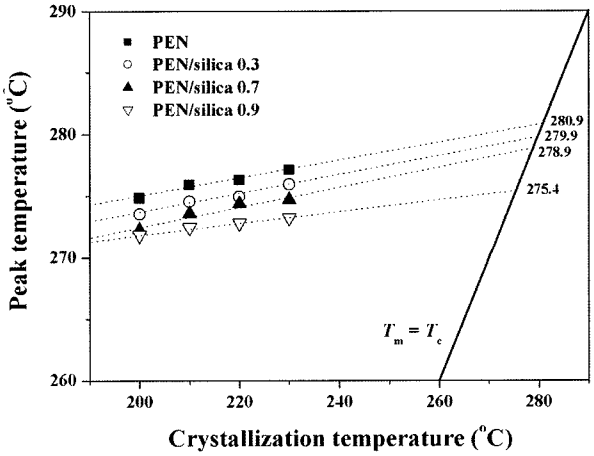

Figure 6. Hoffman-Weeks plots for PEN/silica hybrid nanocomposites as a function of silica content.

which made the formation of perfect spherulites difficult with increasing MMT content.[27] Therefore, the decrease in T_m^0

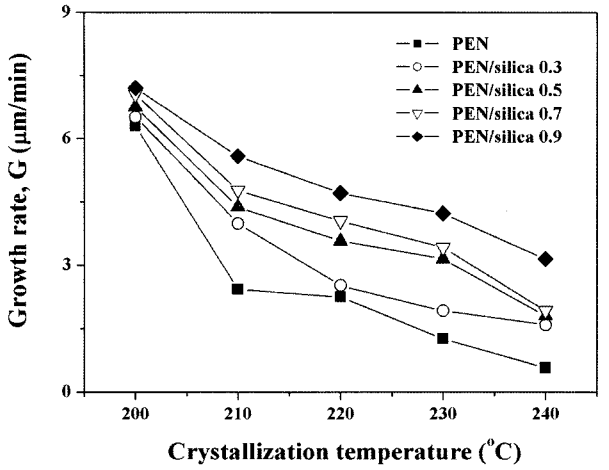

Figure 7. Crystal growth rate for various PEN/silica hybrid nanocomposites as a function of the isothermal crystallization temperature.

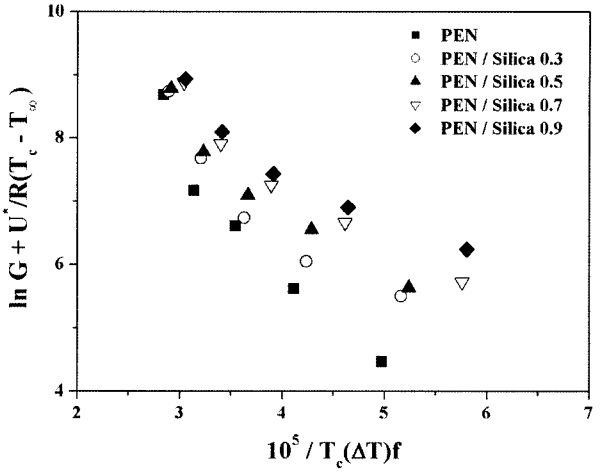

Figure 8. Plots of ln $G + U^*/R(T_c - T_\infty)$ versus $1/T_c(\Delta T)f$ for PEN/silica hybrid nanocomposites.

value with increasing silica content suggests that the crystals in PEN/silica nanocomposites are less perfect than those in pure PEN, a result of the good nucleation effect of the silica nanoparticles in the PEN/silica hybrid nanocomposites.

Secondary Nucleation Theory. The temperature dependence of the linear growth rate of the spherulites can be described by the Laurizen-Hoffman theory for secondary nucleation.[28] Crystal growth rates of the PEN/silica hybrid nanocomposites are shown in Figure 7. It can be seen that the growth rate decreased with increasing crystallization temperature and increased with increasing silica concentration. The effect of silica nanoparticles on the growth rate was characterized using secondary nucleation theory.[28] According to the nucleation theory, the growth rate of polymer crystal, G, at crystallization temperature, T_c, is can be represented as follows:

$$G = G_0 \exp\left[\frac{-U^*}{R(T_c - T_\infty)}\right] \exp\left[\frac{-K_g}{T_c(\Delta T)f}\right] \quad (5)$$

where G_0 is the front factor; U^* is the activation energy for segment diffusion to the site of crystallization; R is the universal gas constant; T_∞ is the hypothetical temperature below which all viscous flow ceases; K_g is the nucleation parameter; ΔT is the degree of supercooling ($\Delta T = T_m^0 - T_c$); T_m^0 is the equilibrium melting temperature, and f is the correction factor given as $2T_c/(T_m^0 + T_c)$. The plot of ln $G + U^*/R(T_c - T_\infty)$ versus $1/T_c(\Delta T)f$ for PEN and the PEN/silica hybrid nanocomposites are shown in Figure 8. As the crystallization kinetics are governed by the nucleation term, the growth rates are insensitive to the U^* and T_∞ values employed in eq. (5).[28,29] In this study, universal values of $U^* = 6{,}300$ J/mol and $T_\infty = T_g - 30$ K were used in all of the calculations.[28-31] With these assumptions, the K_g values can be determined the slope of the plot of ln $G + U^*/R(T_c - T_\infty)$ versus $1/T_c(\Delta T)f$ as shown in Figure 8. It can be seen that the slope of the plots decreased with increasing silica content. The nucleation parameter, K_g, can be expressed by the following equations:

$$K_g = \frac{n\sigma\sigma_e b_0 T_m^o}{\Delta h_f k_B} \quad (6)$$

where σ is the lateral surface energy, σ_e is the fold surface free energy, b_0 is the layer thickness in the direction normal to the growth plane, $\Delta h_f = \Delta H_f \times \rho_c$ is the heat of fusion per unit volume, and k_B is the Boltzmann constant. In this study, the heat of fusion per unit volume (Δh_f) was determined by using the crystal density ($\rho_c = 1.407$ g/cm^3) and the heat of fusion per unit mass ($\Delta H_f = 190$ J/g).[32] In general, values of n are equal to 4 for regime II growth and 2 for regime I or III growth, respectively.[28] The σ_e value for PEN and the PEN/silica hybrid nanocomposites can be estimated using the obtained values of K_g according to the following empirical relations for the lateral surface free energy:[33]

$$\sigma = \alpha(\Delta h_f)(a_0 b_0)^{1/2} \quad (7)$$

where α was derived empirically to be 0.11 by analogy with the well-known behavior of hydrocarbons,[34] and a_0 and b_0 are the monomolecular width and layer thickness, respectively. In this study, values of $a_0 = 0.651$ nm and $b_0 = 0.566$ nm were used in all calculations.[32] The values of K_g and σ_e for the PEN/silica hybrid nanocomposites obtained from eqs. (5)-(7) are shown in Table IV. The values of K_g and σ_e for the PEN/silica hybrid nanocomposites decreased with increasing silica content. The work of chain folding (q) is one of the parameters closely related to the molecular structure, and it's value is apparently proportional to chain stiffness.[28,35,36] The work of chain folding per molecular fold that is required for bending the polymer chain back upon itself, in the appropriate configuration, can be defined as follows:[37]

Table IV. Values of K_g, σ_e, and q for PEN/Silica Hybrid Nanocomposites as a Function of Silica Content

Materials	K_g ($K^2 \times 10^{-5}$)	σ_e (erg/cm^2)	q (J)
PEN	1.82	98.8	7.28×10^{-20}
PEN/silica 0.3	1.35	73.4	5.41×10^{-20}
PEN/silica 0.5	1.25	68.4	5.04×10^{-20}
PEN/silica 0.7	1.08	59.1	4.36×10^{-20}
PEN/silica 0.9	0.92	50.3	3.71×10^{-20}

$$q = 2a_0 b_0 \sigma_e \quad (8)$$

From eq. (8), it can be deduced that the q value is apparently proportional to the $2\sigma_e$. The q values for the PEN/silica hybrid nanocomposites as a function of silica content are shown in Table IV. The q value for PEN was estimated as 7.28×10^{-20} J per molecular chain fold, while that for the PEN/silica 0.9 hybrid nanocomposite was estimated as 3.71×10^{-20} J per molecular chain fold. The q values for the PEN/silica hybrid nanocomposites decreased with increasing silica nanoparticles incorporation, implying that the incorporation of silica nanoparticles has a significant effect on the estimation of the work for chain folding. It can be seen that the smaller the σ_e value, the smaller is the work of chain folding with increasing silica content, indicating that the incorporation of silica nanoparticles lowers the work required in folding the macromolecules in the hybrid nanocomposites. Karayannidis *et al.*[38] reported that the presence of silica nanoparticles decreases the work required for creating a new surface, resulting in higher crystallization rates. Therefore, it can be deduced that the addition of silica nanoparticles as an inorganic nano-scaled reinforcement into the PEN matrix increases the nucleation and crystallization rate of the PEN/silica hybrid nanocomposites, because the silica nanoparticles act effectively as heterogeneous nuclei in the nucleation of crystallization, corresponding with the higher crystallization rate observed, characterized by lower $t_{1/2}$ and higher $\tau_{1/2}$ values.

Dynamic Mechanical Analysis. Dynamic mechanical properties of the PEN/silica hybrid nanocomposites are shown in Figure 9. The incorporation of silica nanoparticles into the PEN matrix improved the modulus of the PEN/silica hybrid nanocomposites below and above T_g, which may be explained by the reinforcing effect of the silica nanoparticles existing in the PEN matrix. For instance, the storage modulus at 30 and 130 °C of the PEN/silica 0.9 hybrid nanocomposite was approximately 4.0 and 0.9 GPa, respectively, 1.2 times and 4.4 times greater than that of PEN. In general, the maximum peak position of tan δ in the plot of tan δ versus temperature can be related to the glass transition temperature.[39] As shown in Figure 9(b), the T_g of the PEN/silica hybrid nanocomposites shifted slightly towards higher temperatures

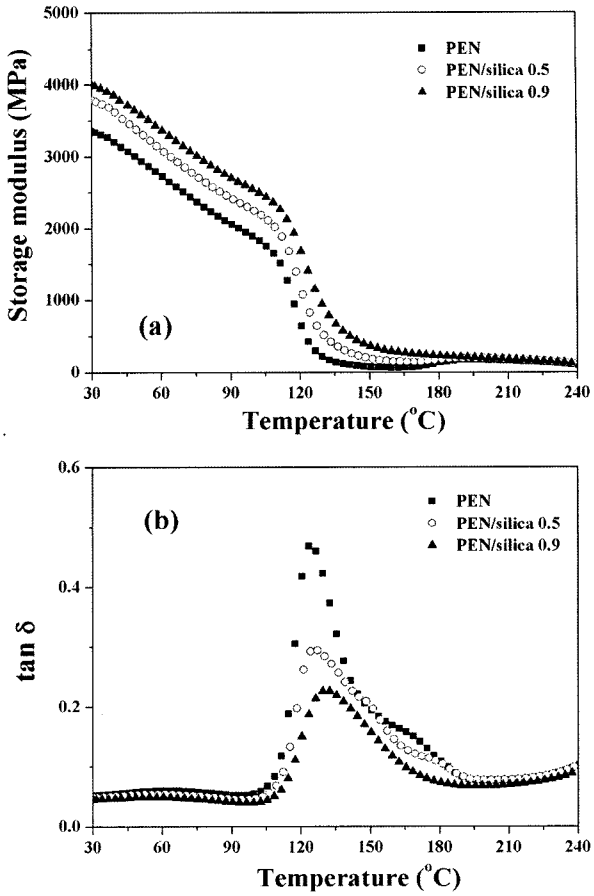

Figure 9. Dynamic mechanical properties of PEN/silica hybrid nanocomposites as a function of temperature: (a) storage modulus and (b) tan δ.

with increasing concentration of silica nanoparticles, implying a decrease in the molecular mobility of the PEN/silica hybrid nanocomposites, caused by some physical interactions between the PEN and the silica nanoparticles due to their high surface area. Similar behavior has also been reported by other researchers in organic/inorganic hybrid nanocomposites.[40-42] The ratio of the storage modulus at 30 °C for the PEN/silica hybrid nanocomposites to that at 130 °C was estimated in order to investigate the effect of silica nanocparticles on the ability to sustain the storage modulus with increasing temperature. As shown in Table V, the modulus ratio was 0.06 for PEN, while it was 0.23 for the PEN/silica 0.9 hybrid nanocomposite. This result indicates that the incorporation of silica nanoparticles enables PEN/silica hybrid nanocomposites to maintain high modulus values at high temperature, compared with PEN. A similar observation has also been reported by Jin *et al.*[43] in the melt-processed carbon nanotube/poly(methyl methacrylate) composite system. SEM microphotograph of the PEN/silica hybrid nanocomposites are shown in Figure 10. Silica nanoparticles randomly dispersed in the PEN matrix exhibited some agglomerated

Table V. Storage Modulus and Modulus Ratio for PEN/Silica Hybrid Nanocomposites as a Function of Silica Content

Materials	Storage Modulus, E' (MPa)		Modulus Ratio ($E'_{130°C}/E'_{30°C}$)
	30 °C	130 °C	
PEN	3353.3	208.6	0.06
PEN/Silica 0.5	3790.2	527.4	0.14
PEN/Silica 0.9	3998.7	922.3	0.23

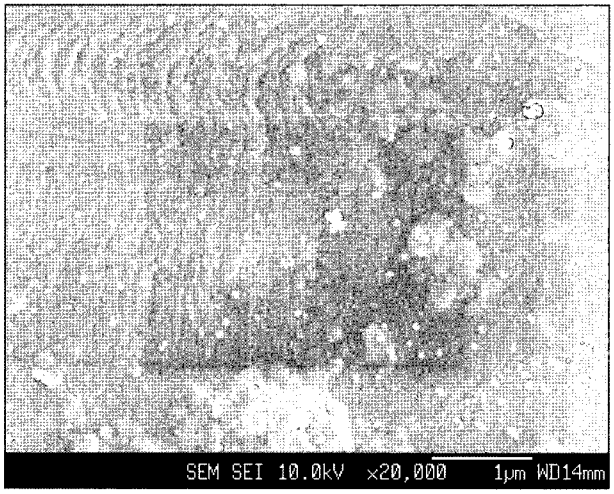

Figure 10. SEM microphotograph of PEN/silica 0.9 hybrid nanocomposites.

structures. However, it can be seen that silica nanoparticles were, on a large scale, uniformly dispersed in the PEN matrix despite some agglomerated particles.

Conclusions

PEN/silica hybrid nanocomposites were prepared using a melt blending process, and the effect of silica nanoparticles on the crystallization and melting behavior of the PEN/silica hybrid nanocomposites was investigated. The incorporation of silica nanoparticles effectively enhances crystallization of the PEN matrix through heterogeneous nucleation, resulting in higher crystallization rates for the PEN/silica hybrid nanocomposites. In addition, the activation energy of crystallization for the PEN/silica hybrid nanocomposites decreased with increasing silica content, indicating that the incorporation of silica nanoparticles induces more heterogeneous nucleation, causing lower activation energy for the PEN/silica hybrid nanocomposites. Double melting behavior observed in the PEN/silica hybrid nanocomposites was attributed to the different lamellae thickness distribution as a result of the melting-recrystallization process occurred during DSC scans. The decrease in the equilibrium melting temperature of the PEN/silica hybrid nanocomposites with increasing silica content suggests that the crystals in the PEN/silica nanocomposites are more imperfect than those of pure PEN, a result of the strong nucleation effect of the silica nanoparticles. The decrease in the values of K_g and σ_e for the PEN/silica hybrid nanocomposites with increasing silica content indicates that the incorporation of silica nanoparticles lowers the work required in folding the macromolecules in the hybrid nanocomposites. The incorporation of silica nanoparticles improved the modulus of the PEN/silica hybrid nanocomposites below and above T_g because of the reinforcing effect of the silica nanoparticles existing in the PEN matrix, enabling the PEN/silica hybrid nanocomposites to maintain high modulus values at high temperature, compared with pure PEN.

Acknowledgements. This research was supported by the Ministry of Education and Human Resources Development directed Hanyang Fusion Materials Capstone Design Program.

References

(1) B. M. Novak, *Adv. Mater.*, **5**, 283 (1993).
(2) T. Lan, P. D. Kaviratna, and T. J. Pinnavaia, *Chem. Mater.*, **6**, 573 (1994).
(3) Y. I. Tien and K. H. Wei, *Macromolecules*, **34**, 9045 (2001).
(4) S. H. Kim, S. H. Ahn, and T. Hirai T. *Polymer*, **44**, 5625 (2003).
(5) S. H. Ahn, S. H. Kim, B. C. Kim, K. B. Shim, and B. G. Cho, *Macromol. Res.*, **12**, 293 (2004).
(6) S. H. Ahn, S. H. Kim, and S. G. Lee, *J. Appl. Polym. Sci.*, **94**, 812 (2004).
(7) J. Z. Alexander, B. Morgan, J. Lamelas, and C. A. Wilkie, *Chem. Mater.*, **13**, 3774 (2001).
(8) F. H. Gojny, J. Nastalczyk, Z. Roslaniec, and K. Schulte, *Chem. Phys. Lett.*, **370**, 820 (2003).
(9) T. J. Pinnavaia and G. W. Beall, *Polymer-Clay Nanocomposites*, Wiley, New York, 2000.
(10) T. D. Fornes, P. J. Yoon, H. Keskkula, and D. R. Paul, *Polymer*, **42**, 9929 (2001).
(11) S. Kumar, H. Doshi, M. Srinivasrao, J. O. Park, and D. A. Schiraldi, *Polymer*, **43**, 1701 (2002).
(12) J. Y. Kim, S. W. Kang, S. H. Kim, B. C. Kim, K. B. Shim, and J. G. Lee, *Macromol. Res.*, **13**, 19 (2005).
(13) J. Y. Kim and S. H. Kim, *J. Polym. Sci.; Part B: Polym. Phys.*, **43**, 3600 (2005).
(14) J. Y. Kim and S. H. Kim, *Polym. Int.*, **55**, 449 (2006).
(15) M. Avrami, *J. Chem. Phys.*, **7**, 1103 (1939).
(16) M. Avrami, *J. Chem. Phys.*, **8**, 212 (1940).
(17) P. H. Cebe and S. D. Hong, *Polymer*, **27**, 1183 (1986).
(18) X. F. Lu and J. N. Hay, *Polymer*, **42**, 9423 (2001).
(19) S. Z. D. Cheng, Z. Q. Wu, and B. Wunderlich, *Macromolecules*, **20**, 2802 (1987).
(20) H. G. Kim and R. E. Robertson, *J. Polym. Sci. Polym. Phys. Ed.*, **36**, 1757 (1998).
(21) D. J. Blundell, *Polymer*, **37**, 1167 (1987).
(22) F. J. Medellin-Rodriguez, P. J. Phillips, and J. S. Lin, *Macromolecules*, **29**, 7491 (1996).

(23) J. Y. Kim, E. S. Seo, S. H. Kim, and T. Kikutani, *Macromol. Res.*, **11**, 62 (2003).
(24) Y. Lee and R. S. Porter, *Macromolecules*, **20**, 1336 (1987).
(25) P. Supaphol, *J. Appl. Polym. Sci.*, **82**, 1083 (2001).
(26) J. D. Hoffman and J. J. Week, *J. Chem. Phys.*, **37**, 1723 (1962).
(27) J. Ma, S. Q. Zhang, Z. Qi, G. Li, and Y. Hu, *J. Appl. Polym. Sci.*, **83**, 1978 (2002).
(28) J. D. Hoffman, G. T. Davis, and J. I. Lauritzen, in *Treatise on Solid State Chemistry: Crystalline and Non-crystalline Solids*, N. B. Hannay, Ed., Plenum Press, New York, 1976, Vol. 3.
(29) J. W. Park, D. K. Kim, and S. S. Im, *Polym. Int.*, **51**, 239 (2002).
(30) W. D. Lee, E. S. Yoo, and S. S. Im, *Polymer*, **44**, 6617 (2003).
(31) S. I. Han, S. W. Kang, B. S. Kim, and S. S. Im, *Adv. Funct. Mater.*, **15**, 367 (2005).
(32) S. Buchner, D. Wiswe, and H. G. Zachmann, *Polymer*, **30**, 480 (1989).
(33) J. Lauritzen and J. D. Hoffmann, *J. Appl. Phys.*, **44**, 4340 (1973).
(34) R. Daubeny, P. De, and C. W. Bunn, *Proc. R. Soc. London A*, **226**, 531 (1954).
(35) A. J. Lovinger, D. D. Davis, and F. J. Padden, *Polymer*, **26**, 1595 (1985).
(36) P. Xing, X. Ai, L. Dong, and Z. Feng, *Macromolecules*, **31**, 6898 (1998).
(37) J. I. Lauritzen and J. D. Hoffman, *J. Res. Natl. Bur. Stand. Sect.*, **64A**, 73 (1960).
(38) G. Z. Papageorgiou, D. S. Achilias, D. N. Bikiaris, and G. P. Karayannidis, *Thermochim. Acta*, **427**, 117 (2005).
(39) K. P. Menard, *Dynamic Mechanical Analysis: A Practical Introduction*, CRC Press, Boca Raton, FL, 1999.
(40) J. D. Lichenhan, *Comments Inorg. Chem.*, **17**, 115 (1995).
(41) P. T. Mather, H. G. Jeon, A. Romo-Uribe, T. S. Haddad, and J. D. Lichenhan, *Macromolecules*, **32**, 1194 (1998).
(42) B. X. Fu, M. Y. Gelfer, B. S. Hsiao, S. Phillips, B. Viers, R. Blanski, and P. Ruth, *Polymer*, **44**, 1499 (2003).
(43) Z. Jin, K. P. Pramoda, G. Xu, and S. H. Goh, *Chem. Phys. Lett.*, **337**, 43 (2001).